

A MICROACTUATOR SYSTEM FOR THE STUDY AND CONTROL OF SCREECH IN HIGH SPEED JETS

Chunchieh Huang¹, Joseph Papp², Khalil Najafi¹, and Hassan M. Nagib²

¹ *Center for Integrated Sensors and Circuits
University of Michigan, 1301 Beal Avenue
Ann Arbor, Michigan 48109-2122*

² *Fluid Dynamics Research Center
Armour College, Illinois Institute of Technology
Chicago, IL 60616*

Abstract

The development of an electrostatic microactuator system for closed-loop control of screech in a high-speed jet flow system is presented in this paper. The electrostatic actuators have been fabricated using a bulk-silicon dissolved-wafer process, and are more than 10 μ m in thickness needed for large stiffness in z -direction. The actuators can resonate at a frequency of about 5kHz, consistent with the "screech" frequency, and an amplitude of 70 μ m peak to peak using 20V dc and 20V ac drive voltage. The system consists of several of these actuators mounted at the exit lip of a high-speed jet flow system and has been shown to provide disturbances in the jet flow measured downstream from the jet nozzle. Closed-loop control strategies and experiments are underway to demonstrate control of screech.

I. Introduction

Development of advanced aircraft requires not only a detailed understanding of the physics of turbulence and fluid dynamics, but also a means to prevent unsteady and potentially dangerous flow conditions. An area of interest in turbulence research is that of "screech" and receptivity of supersonic jets. Screech is a feedback phenomenon which results in the emission of a discrete acoustic tone from supersonic jets operated at off-design conditions [1-3]. The off-design conditions produce a shock cell structure within the jet plume which is required for the existence of screech. The feedback loop consists of shear-layer disturbances convecting through the system of shock cells. Interaction of the disturbances with the shock cells produces acoustic waves that travel upstream outside the shear-layer to the nozzle lip. At the nozzle lip shear-layer disturbances are generated by the acoustic waves through receptivity thus completing the loop. The feedback loop selects and amplifies a single jet instability mode.

By using an array of microactuators it is possible to interfere with the screech feedback loop at the point of receptivity where shear-layer disturbances are created by acoustic waves at the nozzle lip. The microactuator array is designed to effectively replace the original nozzle lip with one that can produce different types of disturbance modes, as shown in Figure 1. Theoretically, the actuator array could then be driven "out of phase" with the fundamental screech instability mode to cancel the screech tone completely.

The frequency of the fundamental screech tone for the one inch nozzle in the High Speed Jet Facility decreases from approximately 9.5 kHz near Mach 1.0 to 4.5 kHz at Mach 1.6. The jet Mach number at which screech experiments would be conducted would therefore determine the resonant frequency of actuator. In addition the smooth decrease in screech frequency is interrupted by regions where no discrete frequency exists and by discontinuous jumps in frequency where a new instability mode becomes the one most amplified.

We have chosen an actuator frequency of 5.0 kHz, which corresponds to a region of smooth change in screech frequency. In addition, this value was chosen to take advantage of one of the discontinuous frequency jumps. Because of the discontinuity, 5.0 kHz actually corresponds to two distinct jet Mach numbers at approximately 1.31 and 1.49. This widens the scope of experimental applications of the actuators by allowing the study of two different jet instability modes. This paper reports the development of a microactuator-microsensor system that can help control and eliminate screech.

II. Actuator Structure

In order to generate sufficient mechanical perturbations into the jet plume at the correct resonant frequency, the actuators should be 1-2mm wide, should not introduce unwanted perturbations (such as thermal) into the jet, should be able to interact with the jet flow by physically penetrating the shear layer, and should be capable of tens of microns of movement at frequencies of 5-8kHz. This requires that the front portion of the actuator tip overhang the edge of its substrate and penetrate the jet flow when activated. These conditions dictate that the actuator be very compliant in the direction parallel to the substrate, and very stiff perpendicular to the substrate. In order to achieve these requirements, electrostatic actuators that are supported by thick, narrow and long beams can be utilized. Electrostatic actuation is desirable because one can achieve relatively large motions in a small area without generating unwanted thermal disturbances. The large thickness required for large stiffness in one direction can be achieved by using thick micromachined bulk silicon microstructures.

Figure 2 shows an overall view of a single actuator. The actuator is fabricated from boron-doped silicon which is supported on a glass substrate [4]. The microstructure is formed

using a high aspect-ratio reactive ion etching process on a silicon wafer that is doped with high concentrations of boron. The silicon wafer is electrostatically bonded to a glass substrate which supports interconnect metal lines, and is dissolved away to leave the microstructure supported on the glass substrate. This will allow for the overhang of the actuator tip. In addition, a large air gap can be formed between the silicon and the glass substrate in order to reduce clamping.

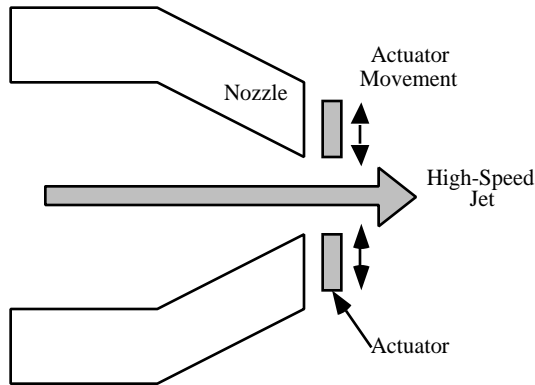


Figure 1: Closed-loop control of screech in a high-speed jet using actuator placed on a jet nozzle.

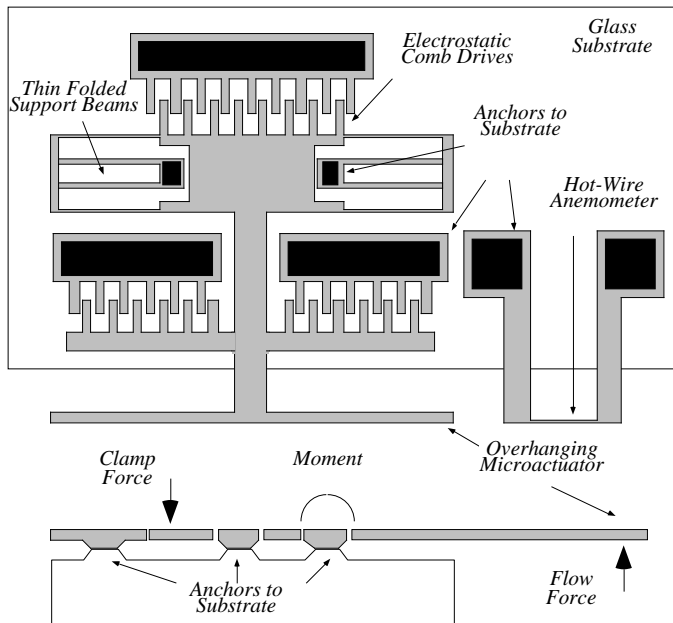


Figure 2: Structure of the electrostatic microactuator.

III. Fabrication

Figure 3 shows the complete dissolved-wafer process which is used to fabricate these actuators. The actuator itself is fabricated from micromachined p++ silicon microstructures that are supported on a glass substrate. The head of the actuator is located in the proper position overhanging the edge of the glass substrate and interacts with the jet flow, as required in this application. The fabrication process of the device requires four masks. It starts by recessing the silicon with KOH to a depth of a few microns, except in areas that will later be bonded to the glass substrate to anchor the actuators. Next an unmasked deep

boron diffusion (~12 μ m) is performed, which defines the thickness of the beams and the teeth of the drive combs. The large thickness is critical to this application since it reduces both the drive voltage and the susceptibility to clamping. The wafer is then patterned and metalized with a Ti/Pt layer. The boron-diffused areas are then etched anisotropically using RIE to pattern the fine microstructures [4]; this completes silicon processing. The glass substrate is patterned and recessed to a depth of about 6 μ m by a mixture of diluted HF and nitric acid to create the bonding anchors. This recess is also critical as it allows the formation of a gap under the silicon structure which is large enough to reduce the clamping of the microactuator to the substrate both during processing and later in operation. The formation of such a gap is practically possible only by using the dissolved wafer process. Glass processing is completed after patterning Ti/Pt/Au interconnect lines on it. Finally, the silicon wafer is electrostatically bonded to the glass wafer, and the sandwich is then immersed in EDP to dissolve away the undoped silicon, leaving the p++ silicon devices mounted on the glass substrate.

Figure 4 shows a SEM view of one of the actuators, and a close-up view of the tip of the actuator overhanging the glass substrate. The device is 1.3mm wide, 10 μ m thick, and has a head that overhangs the glass substrate by ~200 μ m to allow it to enter the jet flow. The length of the folded-beams is 230 μ m and the width is about 4 μ m. The microactuator is driven into resonance electrostatically by large comb drives. Each microactuator can be controlled individually, and can be resonated to an amplitude of larger than 70 μ m peak to peak at a resonant frequency of 5kHz using a 20V ac signal and a 20V dc bias. Note that the microactuator tip is "meshed" with a large number of holes in order to reduce the vertical induced on it by the high speed jet. Table 1 summarizes the measurement results under different bias voltages. Note that the microactuator tip is "meshed" with a large number of holes in order to reduce the vertical forces induced on it by the high speed jet. This will also reduce the possibility of clamping the actuator during operation.

Table 1: Measured results for one actuator.

Bias (ac + dc)	Resonant Frequency (kHz)	Amplitude (μ m p-p)
7.5+7.5	5.18	12
10 + 10	5.16	22
12.5+12.5	5.16	28
15+15	5.16	36
17.5+17.5	5.16	52
20+20	5.16	70

IV. High Speed Jet Facility

The High Speed Jet Facility at the Illinois Institute of Technology Fluid Dynamics Research Center consists of a one inch diameter axisymmetric nozzle exhausting into an anechoic chamber (as shown in Figure 5). The 7,000 ft³ compressed air supply system provides a maximum exit pressure ratio of 14.6 and fully expanded Mach number of 2.4. Jet exit conditions are maintained as supply tank is depleted by a segmented ball control valve and PID digital control loop. Flow conditioning

and two fifth order polynomial contractions within the jet body ensure a high quality laminar exit flow. The anechoic chamber is designed with optical access windows for high-speed shadowgraph and schlieren flow visualization. The jet exit is designed to facilitate the mounting of an array of 16 actuator chips for a total of 32 actuators around inner nozzle diameter.

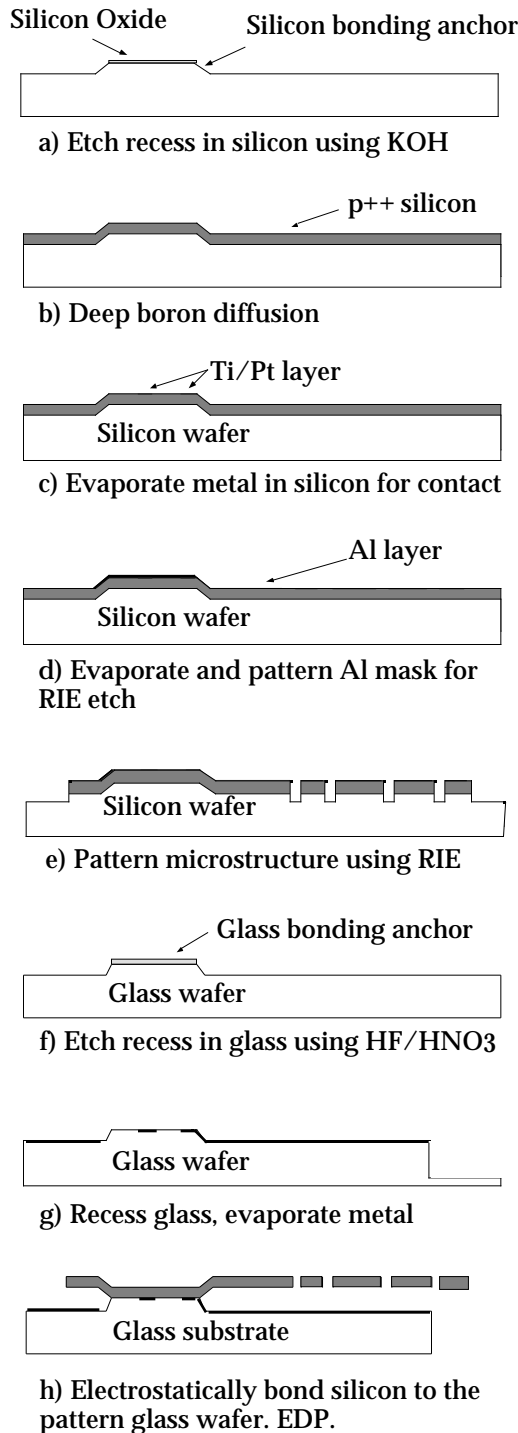


Figure 3: Process sequence for the fabrication of microactuator system using a silicon and a glass wafer with the dissolved wafer process.

Jet exit conditions are determined from stagnation temperature and pressure measurements made in the setting chamber of the jet.

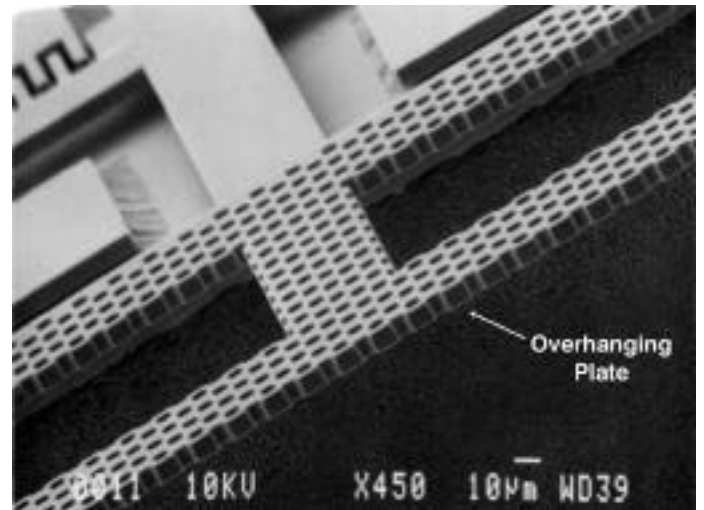
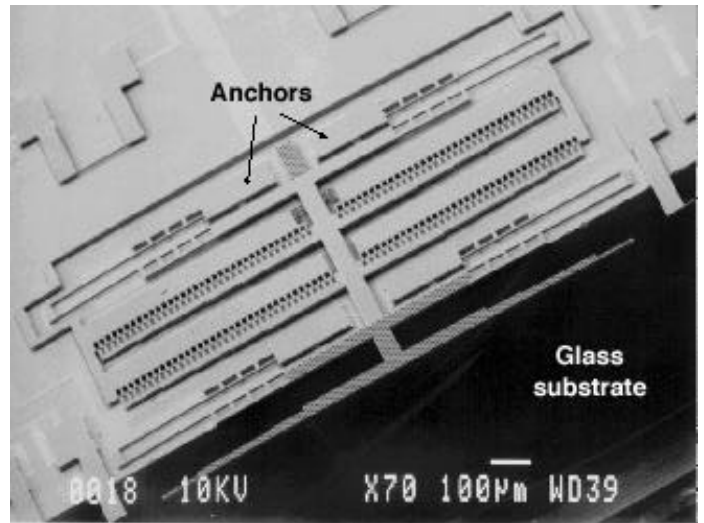


Figure 4: SEM views of the electrostatic actuator designed for controlling screech. The device is 1.3mm wide, 10µm thick. Note that the resonant part is separated from the glass by a distance of about 6µm. A close-up view of the actuator overhung tip is also shown, indicating holes created in it to reduce forces exerted on the actuator by the jet flow.

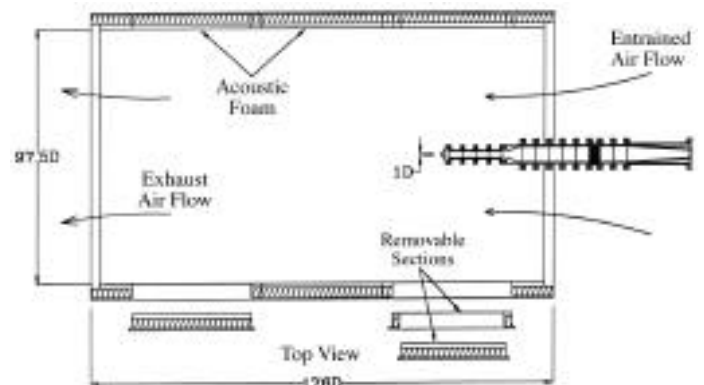


Figure 5: The high-speed jet facility at IIT.

V. Experimental Results

Figure 6 shows the experimental setup for incorporation of the microactuator into the jet facility. It consists of a number of microactuators and hot-wire anemometers that are fabricated on the glass substrate. The glass substrate is attached to a printed circuit board which is then mounted with the microactuator motion aligned radically to the jet's axis in its exit plane on the convergent nozzle of a high-speed jet. Figure 7 shows four actuator chips mounted on printed-circuit boards and attached to the nozzle. These devices have been tested on the high-speed jet facility mentioned above. In order to monitor the operation of the microactuator during testing, a custom-designed circuit which is used to detect the small amplitude of the resonant actuator is attached directly on the back side of each actuator PC board (shown in Figure 8). Figure 9 shows drive and detection electronics and the output voltage from one of these actuators as a function of frequency, showing the resonant peak. As can be seen, a function generator produces the ac signal that is passed through the simple transistor amplifier to generate the necessary high voltage and then fed into one terminal of the actuator. The current from the other terminal of the actuator is fed into a transresistance amplifier which converts the ac current through the actuator into an ac voltage that is picked up externally. Figure 10 shows the shear layer velocity fluctuations generated by an electrostatic actuator and measured by a hot-wire anemometer positioned downstream to the nozzle lip. The actuator used in these experiments did not have the flow-through holes shown in Figure 4. As can be seen, it generates a vibration which travels downstream inside the shear layer at its resonant frequency ($\sim 5\text{kHz}$). However, the actuator can only operate at a jet speed of 25m/s with a distance of $200\mu\text{m}$ between the overhanging plate and the edge of the nozzle lip. It will stop when it is operated at higher jet speeds. Within the supersonic range ($\sim 400\text{m/s}$), it stops operating when it is placed $1\text{-}1.5\text{mm}$ from the edge of the nozzle lip. This we believe is caused by the large moment forces acting on the actuator as it is brought closer to the high-speed jet. These forces can be reduced by a modified design of the actuator system as discussed below.

In Figure 2, a simplified layout of the top and side views of the folded-beam actuator was shown. The higher the jet speed, the larger the force under the overhanging plate becomes. This force may create a moment at the anchors of suspended microstructure and pushes the rear part of the electrostatic comb drives downward to touch the glass substrate. The spring constant of one beam of the folded-beams in the z -direction is given by [5]:

$$k_z = \frac{6EI_{x,b}}{L_b^3} \quad (1)$$

where E is the Young's modulus, L_b is the length of the folded beams, and $I_{x,b}$ is the moment of inertia of the beams. With a beam width of w , thickness of t , the moment of inertia is:

$$I_{x,b} = wt^3/12 \quad (2)$$

Figure 11 shows a schematic illustration of a rigid long plate and four springs attached at points A , A' , B , and B' .

Assuming there is a force F_z under the front end of the plate, it causes a deflection f at the front end, a deflection at the points A , A' , B , and B' , and a deflection r at the rear end. We can easily derive:

$$\frac{f}{r} = \frac{L_2/2}{(L_1 + L_2/2)} \quad (3)$$

$$\frac{f}{r} = \frac{L_2/2}{(L_3 + L_2/2)}$$

Then we can find:

$$f = F_z \frac{(L_1 + L_2/2)}{k_z L_2} \quad (4)$$

and :

$$r = F_z \frac{(L_1 + L_2/2)(L_3 + L_2/2)}{1/2 k_z L_2^2} \quad (5)$$

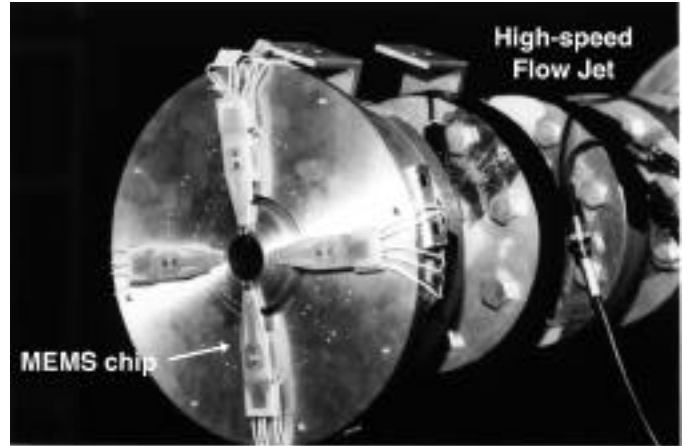


Figure 6: Experimental setup for incorporation of the microactuator into the jet facility, showing the jet nozzle.



Figure 7: Actuator chips mounted on a PC board, which is attached to the front surface of the nozzle. This device has been tested on a high-speed jet facility.

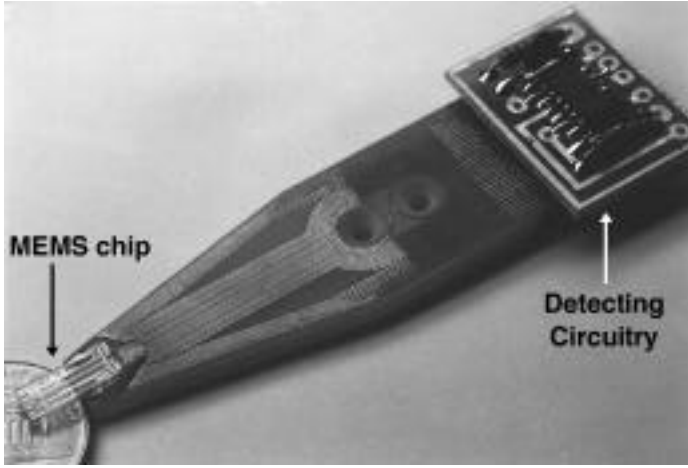


Figure 8: The microactuator chip mounted on a PC board, and the hybrid readout circuitry.

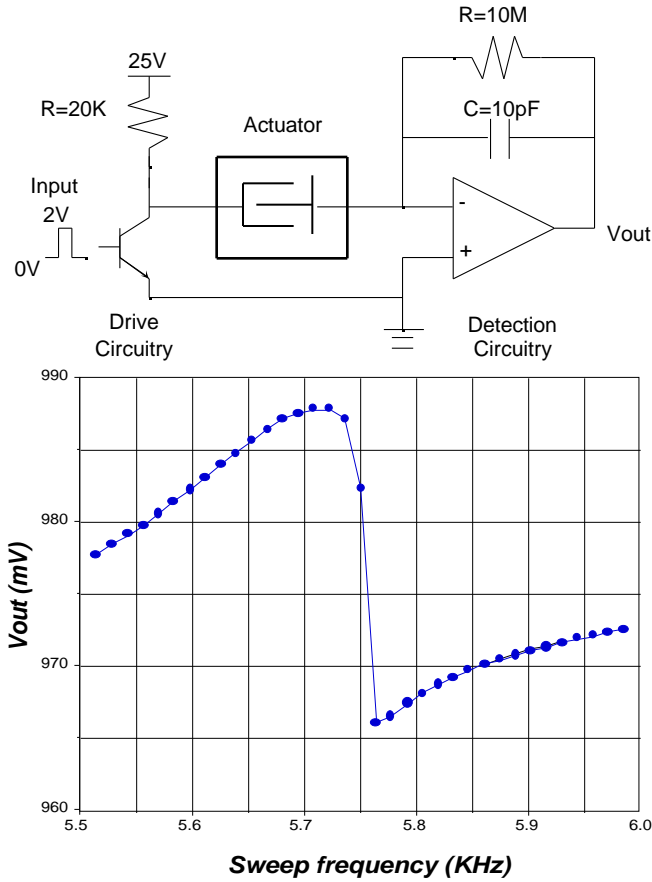


Figure 9: a) Drive and sense electronics for resonating the actuator and detecting the motion. The circuitry is implemented using hybrid electronics. b) Output voltage response from a single actuator driven to resonance.

The maximum deflection at the rear end will be the gap between silicon structure and glass substrate. As can be seen from the equation above, in order to reduce the deflection, we can decrease the length of the plate ($L_1 + L_2 + L_3$), increase the distance L_2 between two anchors without increasing the total length of the plate, or increase the spring constant k_z . From

equations (1) and (2), we can reduce the length of beams, increase its width, or increase the structure's thickness in order to increase k_z ; however, these will also increase the resonant frequency. The shortened plate will significantly reduce the number of electrostatic comb drives; thus reducing the electrostatic force and resonant amplitude. Increasing L_2 , therefore, will be a better way to increase k_z . Figure 4 shows a SEM view of the new actuators. There are two changes in the new design. One is that the anchors are located at two ends of the actuator, instead of in the middle. The other is that we have created holes in the overhanging plate; this produces a smaller F_z . Since there is no truss between two folded beams, the spring constant in x -direction will become [5]:

$$k_x = \frac{48EI_{z,b}}{15L_b^3} \quad (6)$$

In comparison with the original this new design also provides a smaller spring constant in x -direction, as well as a lower resonant frequency. Table 2 compares the old and new designs in terms of the amount of deflection at the rear end as a function of the force exerted on the plate. Assuming the values of k_z and F_z are the same for both designs, the deflection r of the old design is 27 times larger than that of the new actuator. The improvement is even more significant than this because the reduced area of the overhanging plate (due to holes etched in the actuator tip) in the new design results in a smaller F_z , as we mentioned before.

Table 2: Comparison of the torsional stability of the old and new designs for the electrostatic actuator.

	New Design	Old design
L_1 (μm)	250	490
L_2 (μm)	750	135
L_3 (μm)	65	380
$r k_z / F_z$	0.978	27.38

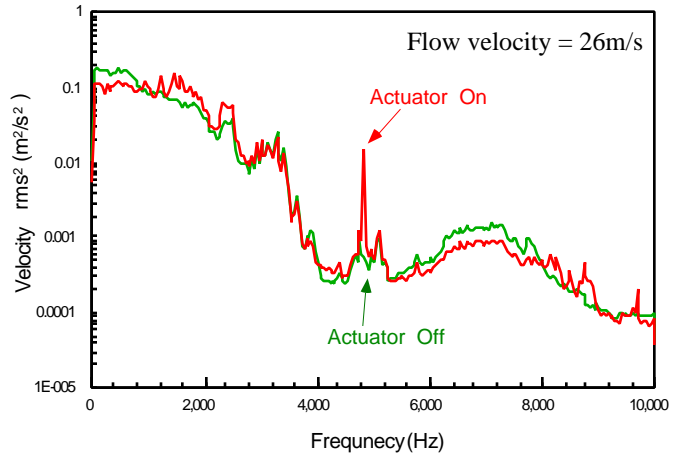


Figure 10: Shear layer velocity fluctuations measured by a hot-wire positioned 9mm downstream to the nozzle lip. As can be seen, the actuator generates a disturbance at its resonant frequency ($\sim 5\text{kHz}$), which travels downstream inside the shear layer.

Acknowledgments

The authors would like to thank Mr. Emad J. Alnajjar and the staff at the Illinois Institute of Technology Fluid Dynamics Research Center for help in the testing in high speed jet. This work was sponsored by the Air Force Office of Scientific Research under contract #F49620-94-0184.

References

- [1] D.W. Bechert, and B. Stahl, "Shear Layer Excitation, Equipment vs. Theory," DFVLR TR No. DFVLR-FB pp. 84-26, 1984
- [2] D.G. Crighton, "The Kutta Condition in Unsteady Flow," *Ann. Rev. Fluid Mech.*, 17, pp. 411-445, 1985
- [3] R.E. Drubka, P. Reisenthel, and H.M. Nagib, "The Dynamics of Low Initial Disturbance Turbulent Jets," *Phys. Fluids A*, 1, pp. 1723-1735, 1989
- [4] Y.B. Gianchandani, and K. Najafi, "A Bulk Silicon Dissolved Wafer Process for Microelectromechanical Systems," *IEEE/ASME J. Micro Electro Mechanical Systems*, Vol. 1, No. 2, pp. 77-85, June 1992
- [5] G.K. Fedder, "Simulation of microelectromechanical systems", Ph.D. Dissertation, University of California at Berkeley, 1994.

The new microactuators are being tested on the jet facility and will be used to demonstrate full control of screech at even higher jet speeds. The initial experiments with the old microactuators have been very promising in that they have demonstrated that rather large disturbances can be generated downstream from the jet nozzle using small perturbations introduced in the jet at the nozzle opening using miniature microactuators. In many applications, it is also desirable to have hot wire anemometers with which one can measure flow velocity in the vicinity of the microactuators.

The microactuator chips fabricated here also contain an array of hot wire anemometers. Figure 12 shows an SEM view of a hot wire fabricated from p++ silicon. The hot wire is supported on the same glass substrate, which provides an ideal thermally insulating substrate for it. The hot wire shown here is 100 μm long, 12 μm thick, and 4 μm wide, and provides a sensitivity of about 1 mV/m/sec. The substrate contains a total of 23 hot wires, dispersed around the chip, with some overhanging the glass substrate to measure flow velocity close to the jet. These hot wires are very important in that they provide high spatial resolution, higher sensitivity, and good frequency response due to the high thermal resistance provided by the glass substrate.

VI. Conclusion

We have fabricated a microactuator-microsensor system for the study and control of screech in high-speed jets. This system contains an array of small microactuators and hot-wire anemometers fabricated using p++ bulk-silicon dissolved wafer process. The devices have operated as designed and actuation amplitudes of at least 70 μm peak to peak at frequencies around 5kHz. In addition, a custom-designed circuit board has been developed for monitoring the operation of the micromechanical system *in-situ* during actual use on a high-speed jet flow (HSJF). The microactuators have been tested on the HSJF, and have demonstrated that disturbances can be introduced into a high-speed jet by introducing perturbations at the jet nozzle using microactuators. New improved microactuators have been also developed to increase the resistance of the microactuator to clamping at high jet speeds.

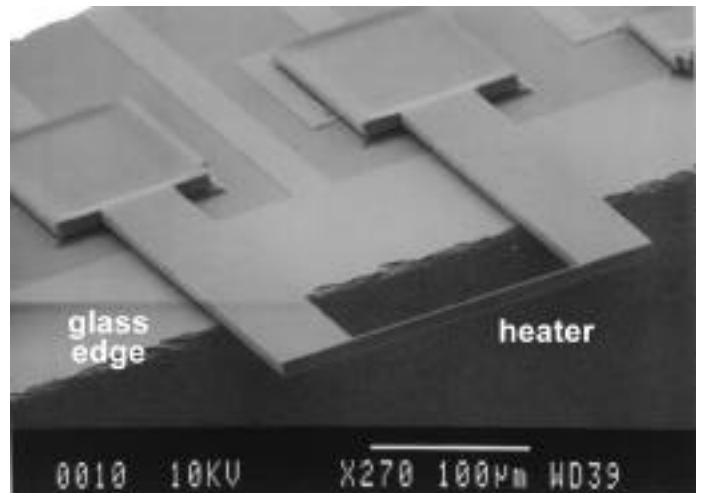


Figure 12: SEM view of a hot wire anemometer integrated with microactuators. The hot wire is fabricated using p++ silicon and provides a sensitivity of about 1mV/m/sec.

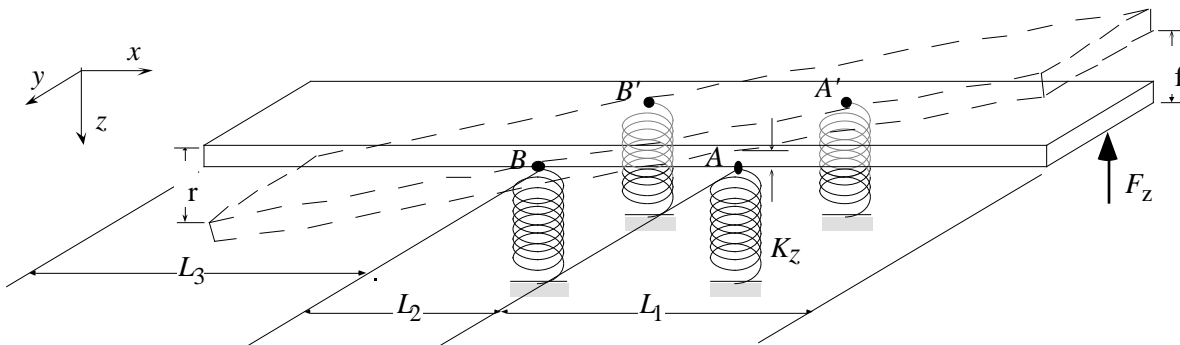


Figure 11: A rigid plate with four spring in z -direction. A force, F_z , at the front end of the plate represents the flow force of high speed jet.